Interference Suppression via Operating Frequency Selection

Richard M. Davis, *Senior Member, IEEE*, Ronald L. Fante, *Fellow, IEEE*, Thomas P. Guella, and Robert J. Balla

***Abstract*— Spectral analysis of the environment, often called sniffing, is used to find a clear operating band in radar and communication systems. In this paper, the authors show that the sniffing technique can be used to null multiple broad-band sidelobe jammers by exploiting the transfer function of the antenna. Analysis and computer simulation are used to demonstrate performance.**

***Index Terms*— Jamming, radar, suitting.**

I. Introduction

ELECTRONIC protection against mainlobe and sidelobe jamming and nonhostile interference begins with environment sensing. One of the most powerful sensing tests entails performing a spectral analysis of the environment—also referred to as sniffing. The sniffing technique is used to find a clear region within the tunable bandwidth of a radar or communication system. In addition to finding clear bands or dips in the radiated power spectrum of friendly or hostile interferers, the sniffer can find nulls introduced by the transfer function of the receiving antenna. The sniffing test can be made to function like a sidelobe canceller by picking the operating frequency which places multiple broad-band jammers in or near sidelobe nulls. The test can be implemented by making power measurements at equally spaced intervals across the tunable band at the output port of the antenna. The frequency corresponding to the lowest power measurement is used for transmission. The test should be made within about one second before transmission and should be repeated for every beam pointing direction. The sniffing test has historically not been implemented in every beam pointing direction and the measurements have not always been made at the output port of the antenna.

It is well known that antenna patterns of phased arrays scan with frequency. Each frequency within the spectrum of a wide-band interferer is received with a slightly different gain. The spectrum of a sidelobe interferer traces out the sidelobe pattern of the antenna in the angular region surrounding its direction of arrival. A jammer power spectrum, which is white (flat) upon entering the antenna, will be colored (in this case serrated) at the output of the antenna. The output spectrum will be the product of the jammer spectrum with the transfer (filter) function of the antenna. If the jammer operates in a wide-band mode, and spreads its energy over the entire tunable bandwidth of the radar or communication system, the filter function of the antenna will introduce nulls and dips in the jammer's spectrum. The nulls can then be located using the sniffer. If the system transmits over a narrow bandwidth on a frequency corresponding to one of the nulls, the jammer will fall in the null and be cancelled. Although the jammer rejection capability of the sniffer degrades in the presence of multiple interferers, analysis and computer simulation show that the degradation is graceful. In effect, the sniffer acts like a sidelobe canceller having limited capability against a small number of broad-band interferers. Sniffing does not support as much cancellation as adaptive nulling, but requires no additional receivers or correlation processing. It can be used in addition to adaptive nulling. The sniffing technique exploits the frequency agility capability of modern radars.

Petrocchi *et al.* [1] appear to be among the first to recognize that an antenna pattern can turn a white noise sidelobe jammer into a colored noise jammer having nulls in its spectrum and that the colored spectrum can be exploited by a frequency agile radar. Strappaveccia [2] proposed using a separate receiver to sample the power at a number of frequencies at the output of the beamformer in a mechanically rotating antenna, to minimize the power received from a single sidelobe jammer. In this paper, the technique is applied to phase and time-steered arrays and a theory is developed to show that it can be used to null multiple sidelobe jammers. Computer simulation is used to support the analysis.

II. Analysis

A. Operational Concept

The sniffer is an environment sensing technique that can be used to find an operating band having minimum electromagnetic interference within the tunable bandwidth of a radar or communication system. Wide-band sidelobe interferers spread their energy through the sidelobes in the region surrounding their direction of arrival. The sniffer attempts to find a narrow operating band over which all of the interferers are in or near a null. Implementation entails looking ahead in each beam and cycling through many (N_f) frequencies roughly equally spaced across the tunable band. A power measurement is made in a narrow sampling band (B_s) at each frequency and the band having minimum interference is chosen for transmission. Ideally, the sampling bandwidth would be set equal to the instantaneous bandwidth to be used when transmitting in the designated beam. The technique will be most effective when

Manuscript received December 29, 1997; revised June 30, 1998.

R. M. Davis, R. L. Fante, and T. P. Guella are with the MITRE Corp., Bedford, MA 01730–1420 USA.

R. J. Balla is with the U.S. Army Space and Missile Defense Command, Hunstville, AL 35807 USA.

Publisher Item Identifier S 0018-926X(99)04769-9.

0018–926X/99$10.00 © 1999 IEEE

the radar is operating with narrow-band waveforms (fractional bandwidths less than 1%). The power measurement at a particular frequency f_i, in the presence of N_j equal power wide-band jammers, can be represented mathematically as

$$P(f_i) = P_n + J_o \sum_{j=1}^{N_j} \int_{f_i - B_s/2}^{f_i + B_s/2} |g(f, \alpha_j, \beta_j)|^2 \, df \quad (1)$$

where:

P_n	receiver noise power in sampling bandwidth;
J_o	power spectral density of jammer received with isotropic gain;
$g(f, \alpha_j, \beta_j)$	voltage gain of antenna in the angular direction (α_j, β_j) at frequency f.

The way in which the sniffer technique is implemented will depend upon whether or not time-delay steering is available. Time steering is used on phased arrays to prevent excessive signal loss when operating over wide bandwidths. Changing frequency causes shifts in the mainbeam pointing direction. The problem is easily solved in the case of narrow-band operation by changing the element phase shifter settings to compensate for the shift in frequency. In the case of wide-band operation, time-delay steering must be used to prevent the beam from scanning. The loss can usually be held to acceptable levels by implementing time steering at the subarray level.

If time-delay steering is available, the sniffer can be implemented by steering the array to a particular pointing direction and cycling through the frequencies while keeping the phase shifter settings fixed. This approach only requires changing the local oscillator setting and making a power measurement at each setting. The authors simulated the sniffer on a computer for an array which used time-delay steering at the subarray level. It was found that a small signal loss occurred due to the subarrays scanning with frequency when the local oscillator was stepped without changing the phase shifters. The loss varied from 0.0 to 0.7 dB as the beam pointing direction was varied from 0.0 to 45.0° off array normal.

If time-delay steering is not available, then the phase shifter setting for each element in the array will have to be recalculated at a number (but not all) of equally spaced frequencies across the tunable band. The same phase shifter setting used during sniffing must be used when the beam is actively interrogated. The required power measurements can be made by stepping the local oscillator to frequencies surrounding each frequency at which the phase shifters were reset. Since the signals to be measured could be jammer random processes, a number of independent samples (see Section II-C) must be taken at each frequency to estimate the mean receive power.

Implementation requires scheduling a passive dwell within about one second prior to transmitting in each beam position in order to make the power measurements at N_f frequencies across the tunable band. If time-delay steering is available, the time required for the passive dwell is

$$T_{\text{dwell}} = N_{\text{freq}}(N_{\text{sample}} \times T_{\text{sample}} + T_{\text{osc}}) \quad (2)$$

where:

N_{sample}	number of power samples made at a given frequency;
T_{sample}	analog to digital converter sample time;
T_{osc}	time to change local oscillator to next frequency setting.

If time-delay steering is not available and the phase shifters must be changed at each frequency, (2) may have to be modified. If the time required to change the phase shifters (T_{shift}) is larger than T_{osc}, then T_{osc} must be replaced with T_{shift}. The total time needed to perform the passive dwells in all beam pointing directions, in an array which used time-delay steering at the subarray level, was found to typically amount to 1–2% of the total available (transmit plus receive) time. The performance of the sniffer will degrade if the jammers move a significant fraction of a sidelobe between sniffing and transmission. The degradation places a limit on the allowable time (ΔT) between sniffing and transmission. ΔT depends upon the range (R) and velocity (V) of the jammer platform, in addition to the allowable angular displacement $(\Delta\theta)$. In particular

$$\Delta T < \left(\frac{R}{V}\right)\Delta\theta. \quad (3)$$

Our simulation results predict that the nulling performance will be degraded by 3 dB if $\Delta\theta$ equals approximately one-tenth of a sidelobe.

Although the best performance will occur for single beam systems, the technique can be extended to include multiple beams. In a tracking radar, for example, we may want to minimize the interference in the sum and difference beams. The power to be minimized in the latter case would be

$$P_d(f_i) = 2P_n + J_o \sum_{j=1}^{N_j} \int_{f_i - B_s/2}^{f_i + B_s/2} (|g_\Sigma(f, \alpha_j, \beta_j)|^2 + |g_\Delta(f, \alpha_j, \beta_j)|^2) \, df \quad (4)$$

where

$g_\Sigma, g_\Delta =$ voltage gains in sum and difference antenna patterns.

B. Frequency Scanning of Phased Arrays in Sidelobe Directions

A null or dip in the power spectrum of the electromagnetic interference can be introduced at the source of the interference, can be due to multipath, or can be introduced by the receiving antenna. Our focus is on the receiving antenna. Therefore, we consider a single white noise sidelobe interferer that radiates energy uniformly over the tunable bandwidth of the radar. We wish to calculate the number of sidelobes that the interferer occupies, and for simplicity, we have limited the analysis to linear arrays.

The phase of a cw signal at frequency f arriving at an angle θ relative to array normal in the nth element of a linear array is given by (5) for an array phase steered to θ_0 at frequency f'

$$\phi_n(f, \theta, f', \theta_0) = \frac{2\pi f n d \sin\theta}{c} + \psi_n(f', \theta_0) \quad (5)$$

where:

ψ_n phase shifter settings on nth element in array; $= \dfrac{-2\pi f' n d \sin\theta_0}{c}$;

d element spacing;

f' operating frequency at which phase shifter settings are calculated.

Assuming the phase shifters are not changed, the pattern shift $(\Delta\theta)$ at an angle θ_1 due to a frequency shift from f_1 to f_2 can be obtained by solving

$$\phi_n(f_1, \theta_1, f', \theta_0) = \phi_n(f_2, \theta_2, f', \theta_0) \tag{6}$$

for $\Delta\theta = \theta_2 - \theta_1$. Using (5)

$$\frac{2\pi f_1 n d \sin\theta_1}{c} = \frac{2\pi f_2 n d \sin(\theta_1 + \Delta\theta)}{c}. \tag{7}$$

Assuming

$$\sin(\theta_1 + \Delta\theta) = \sin\theta_1 + \Delta\theta\cos\theta_1 \tag{8}$$

$$\begin{aligned}\Delta\theta &= \left(\frac{f_1 - f_2}{f_2}\right)\frac{\sin\theta_1}{\cos\theta_1} \\ &= (f_1 - f_2)\left(\frac{D\sin\theta_1}{c}\right)\left(\frac{\lambda_2}{D\cos\theta_1}\right) \\ &= BT\theta_3\end{aligned} \tag{9}$$

where:

B $= f_1 - f_2$;

T difference in arrival time of the plane wave across array face $= \dfrac{D\sin\theta_1}{c}$;

D diameter of array;

θ_3 3-dB beamwidth at $\theta_1 = \dfrac{\lambda_2}{D\cos\theta_1}$.

Equation (9) shows that the pattern shift at angle θ_1 due to a frequency change B is equal to the time-bandwidth product measured in sidelobes where time is the difference in arrival time of the interferer's plane wave across the array face and bandwidth is the spectrum over which the interferer spreads its energy.

In large phase steered arrays, it will be necessary to change the phase shifter settings whenever significant changes are made in the operating frequency to prevent the beam pointing direction from changing. Assuming that the phase shifter setting on the nth element is changed from $2\pi f_1 n d \sin\theta_0/c$ to $2\pi f_2 n d \sin\theta_0/c$ as frequency is changed from f_1 to f_2 (note that in this case $f_1' = f_1$ and $f_2' = f_2$), the pattern shift in the direction of a sidelobe jammer located at θ_1 can be obtained by solving (10) for $\Delta\theta = \theta_2 - \theta_1$

$$\phi_n(f_1, \theta_1, f_1, \theta_0) = \phi_n(f_2, \theta_2, f_2, \theta_0). \tag{10}$$

Using (5) and (8)

$$\begin{aligned}&\frac{2\pi f_1 n d \sin\theta_1}{c} - \frac{2\pi f_1 n d \sin\theta_0}{c} \\ &\quad = \frac{2\pi f_2 n d \sin\theta_2}{c} - \frac{2\pi f_2 n d \sin\theta_0}{c}.\end{aligned} \tag{11}$$

and

$$\Delta\theta = (f_1 - f_2)\left(\frac{D(\sin\theta_1 - \sin\theta_0)}{c}\right)\left(\frac{\lambda_2}{D\cos\theta_1}\right) = BT'\theta_3 \tag{12}$$

where

$$T' = \frac{D(\sin\theta_1 - \sin\theta_0)}{c}.$$

The pattern shift as measured in sidelobes is observed to still be equal to the time-bandwidth product, but now time must be interpreted as the difference in arrival time across the array face assuming the array had been time-delay steered to θ_0. In other words an array in which the phase shifters are changed each time frequency is changed (to prevent the beam pointing direction from changing), and operates over a narrow bandwidth, will behave like an array which is time steered. If the array utilizes time steering, the phase shifters need not be changed each time the local oscillator is stepped when implementing the sniffing technique to make the required power measurements. Changing frequency will not scan the beam in a time steered array. If time steering is implemented at the subarray level, there will, as previously noted, be a small loss in signal due to the subarrays scanning with frequency.

Equation (12) predicts that the sniffing technique should be able to find BT' narrow bands in which a wide-band interferer falls in a sidelobe null. The phenomenon is demonstrated pictorially in Fig. 1. The top insert shows the CW pattern of a 100-element C-band array with element spacing of $0.58\lambda_o$ steered 20° off array normal. The bottom inserts show frequency transfer functions of the array at 60° with (bottom insert) and without (center insert) changing the phase shifter settings at each frequency. In large arrays (such as the one used in this example) the phase shifters would have to be changed each time the frequency is changed to prevent the beam pointing direction from shifting. In this example, the sniffer would have five nulls to choose from that would place the interferer in a null. If the array had been steered to array normal, BT' would be equal to BT and the sniffer would have eight nulls to choose from.

C. Number of Power Samples Required at Each Frequency

Since the interfering waveforms may be random processes, the question arises regarding how many samples are needed to obtain an estimate of the interference-to-noise ratio. In this section we study how many samples (L) are required at each sniffed frequency, to obtain a good estimate of the mean interference power. That is, how large must L be such that the statistic

$$S = \frac{1}{L}\sum_{\ell=1}^{L} |V_\ell|^2 \tag{13}$$

is a good approximation to $\langle |V|^2 \rangle$, where

$$V_\ell = \sum_{m=1}^{M} v_{m\ell} g(f, \theta_m) + \eta_\ell \tag{14}$$

and $\langle\,\rangle$ denotes expectation. $v_{m\ell}$ is the voltage due to the mth interferer at the ℓth time sample (or range bin), $g(f, \theta)$ is the voltage gain of a linear array at frequency f and angle θ relative to array normal, and η_ℓ is the receiver noise thermal voltage at the ℓth sample time. In the analysis to follow,

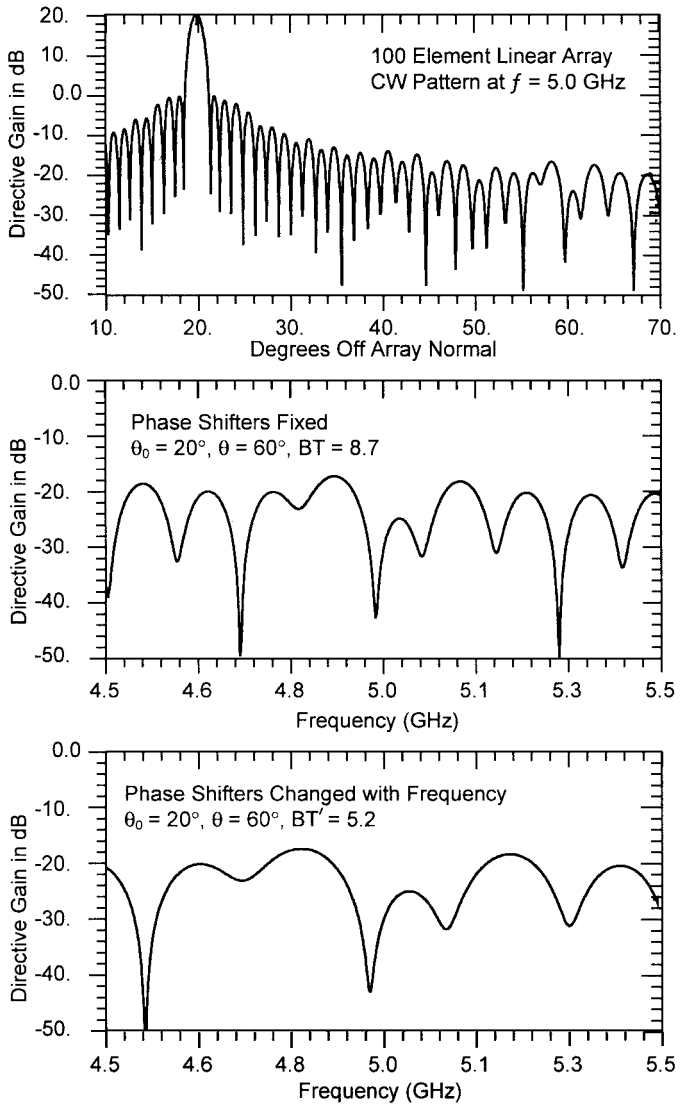

Fig. 1. Frequency transfer functions of 100 element linear array with and without changing phase shifter settings.

we derive the probability density and cumulative distribution functions for the statistic S.

Let us define the phase reference so that $g(f,\theta)$ is real, and then decompose V_ℓ into its in-phase and quadrature components as

$$I_\ell = \sum_{m=1}^{M} x_{m\ell} g(f,\theta_m) + x'_\ell \tag{15}$$

$$Q_\ell = \sum_{m=1}^{M} y_{m\ell} g(f,\theta_m) + y'_\ell \tag{16}$$

where $v_{m\ell} = x_{m\ell} + iy_{m\ell}$ and $\eta_\ell = x'_\ell + iy'_\ell$.

If the interferer and noise voltages are zero mean Gaussian random processes, it is evident that

$$\langle I_\ell \rangle = \langle Q_\ell \rangle = 0 \tag{17}$$

$$\langle I_\ell Q_\ell \rangle = 0 \tag{18}$$

$$\langle I_\ell^2 \rangle = \langle Q_\ell^2 \rangle = \sum_{m=1}^{M} |g(f,\theta_m)|^2 \sigma_J^2 + \sigma_n^2 \tag{19}$$

where

$$\sigma_J^2 = \langle x_{m\ell}^2 \rangle = \langle y_{m\ell}^2 \rangle \tag{20a}$$

$$\sigma_n^2 = \langle x_\ell'^2 \rangle = \langle y_\ell'^2 \rangle. \tag{20b}$$

Thus, (13) can be rewritten as

$$S = \frac{1}{L} \sum_{\ell=1}^{L} (I_\ell^2 + Q_\ell^2) \tag{21}$$

where I_ℓ and Q_ℓ are Gaussian random variables. If we assume that the time samples are spaced by greater than $1/B_s$, where B_s is the sampling bandwidth over which the power measurements are made, then all I_ℓ, Q_ℓ are uncorrelated.

Now define

$$\begin{aligned} v_\ell &= I_\ell^2, && \text{for } \ell = 1 \text{ to } L \\ &= Q_\ell^2, && \text{for } \ell = L+1 \text{ to } 2L. \end{aligned} \tag{22}$$

Then, (21) can be written as

$$S = \frac{1}{L} \sum_{\ell=1}^{2L} v_\ell. \tag{23}$$

Because I_ℓ and Q_ℓ are Gaussian random variables, v_ℓ has probability density

$$\begin{aligned} p_v(v_\ell) &= \frac{1}{\sqrt{2\pi v_\ell}} \exp\Big(-\frac{v_\ell}{2\sigma^2}\Big), && \text{for } V_\ell \geq 0 \\ &= 0, && \text{for } V_\ell < 0 \end{aligned} \tag{24}$$

where

$$\sigma^2 = \sigma_J^2 \sum_{m=1}^{M} |g(f,\theta_m)|^2 + \sigma_n^2. \tag{25}$$

The probability density satisfied by S is determined from the probability density satisfied by v by using characteristic functions. The characteristic function of v is

$$M_v(x) = \int_0^\infty dv\, p(v) e^{-jvx} = \frac{1}{\sqrt{2\sigma}} \left(\frac{1}{2\sigma^2} + jx \right)^{-\frac{1}{2}}. \tag{26}$$

Since I_ℓ and Q_ℓ are independent, the characteristic function of S is $M_v(x)$ raised to the $2L$ power. Taking the inverse Fourier transform of the resulting characteristic function gives the probability density of S as

$$\begin{aligned} p_s(S) &= \frac{L^L S^{L-1} \exp\big(-\frac{LS}{2\sigma^2}\big)}{2^L \sigma^{2L} \Gamma(L)}, && \text{for } S \geq 0 \\ &= 0, && \text{for } S < 0 \end{aligned} \tag{27}$$

where $\Gamma(x)$ = Gamma Function of x. Equation (27) is a chi-squared distribution with moments

$$\langle S \rangle = 2\sigma^2 \tag{28}$$

$$\langle S^2 \rangle = 2\sigma^2 \left(1 + \frac{1}{L} \right). \tag{29}$$

Using (27) we can calculate the probability that S lies within $\pm\varepsilon$ of the true mean given by $\langle S \rangle$.

$$\text{Prob} = \frac{L^L}{2^L \sigma^{2L} \Gamma(L)} \int_{\langle S \rangle (1-\varepsilon)}^{\langle S \rangle (1+\varepsilon)} dS\, S^{L-1} \exp\left(\frac{-LS}{2\sigma^2} \right). \tag{30}$$

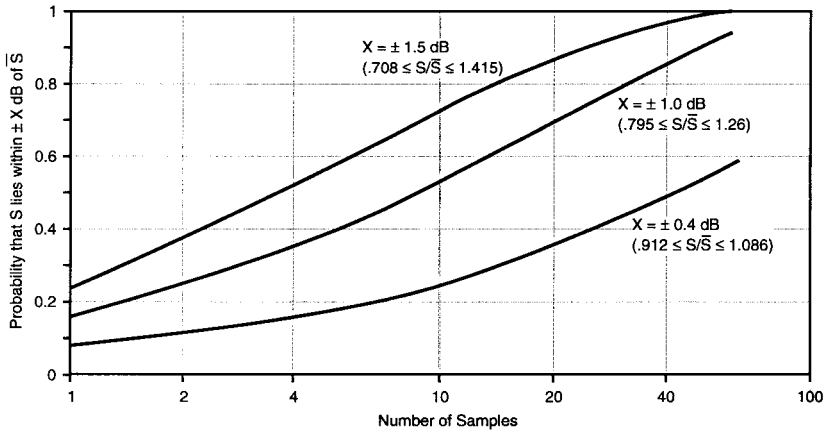

Fig. 2. Probability that estimator for power at a particular frequency is within X dB of true mean.

If we use (28), and define $\tau = LS/2\sigma^2 = LS/\langle S\rangle$, we obtain

$$\text{Prob} = \frac{1}{\Gamma(L)} \int_{L(1-\varepsilon)}^{L(1+\varepsilon)} d\tau\, \tau^{L-1} \exp(-\tau). \tag{31}$$

Equation (31) has been evaluated and the result plotted in Fig. 2. The figure shows that if 50 samples are used to estimate $\langle S\rangle$ there is a 0.99 probability that the result will be within 1.5 dB of $\langle S\rangle$. If we use 20 samples to estimate $\langle S\rangle$, there is a probability of 0.87 that the result will be within 1.5 dB of $\langle S\rangle$ and 0.7 that it will be within 1.0 dB.

D. Theoretical Performance: A Narrow-Band Analysis

In this section, we derive a formula for the expected reduction in jamming power due to the sniffer as a function of the number of sniffed frequencies and the number of sidelobe jammers present. The analysis is based upon the idea that the number of frequencies which must be sampled to reduce the power of an interferer by ε should be roughly equal to the inverse of the probability that the sidelobe gain on the interferer is ε times lower than the root mean square (rms) sidelobe gain. In the analysis to follow, we derive the probability density function for $\varepsilon M\bar{Z}$, where M is the number of equal power jammers and $\bar{Z}$ is the average received power of each jammer at the beamformer output. All jammers are assumed to have the same power and to spread their energy uniformly over the tunable bandwidth (B) of the radar.

When M jammers are present in the sidelobes of an array the received interference power at frequency f, averaged over many range cells, is

$$R(f) = \sum_{m=1}^{M} J_m Z_m + \sigma^2 \tag{32}$$

where

$$Z_m = |g(f,\theta_m)|^2. \tag{33}$$

J_m is the mean square power of the mth jammer random process, θ_m is the azimuth of the mth jammer, σ^2 is the receiver noise power and $g(f,\theta)$ is the normalized voltage gain of the antenna at frequency f and azimuth θ. All range dependent effects are assumed to be normalized out. It should also be noted that (32) is for narrow-band radar operation, i.e., the analysis assumes that the sampling bandwidth (B_s) is zero. For wide-band operation $|g(f,\theta_m)|^2$ must be integrated over B_s. The interference power $\bar{R}$ averaged over the entire sniffed frequency band B is, therefore

$$\bar{R} = \sum_{m=1}^{M} J_m \bar{Z}_m + \sigma^2 \tag{34}$$

where

$$\bar{Z}_m = \frac{1}{B} \int_{f_0-\frac{B}{2}}^{f_0+\frac{B}{2}} |g(f,\theta_m)|^2\, df \tag{35}$$

and f_0 is the carrier frequency.

Now if the sidelobes are error dominated it is well known that for a given frequency f, the voltage amplitude is a Rayleigh-distributed random variable and the power function Z_m is an exponentially-distributed random variable. That is, the probability density function for Z_m is

$$p_z(Z_m) = \frac{1}{\langle Z_m\rangle} \exp\left(-\frac{Z_m}{\langle Z_m\rangle}\right) \tag{36}$$

If the bandwidth B is sufficiently large that many zeros of $g(f,\theta)$ are encompassed by the range $f_0 - B/2 \le f \le f_0 + B/2$ (or equivalently $BT \gg 1.0$, see Section II-B) then we may use the approximation

$$\langle Z_m\rangle \approx \bar{Z}_m \approx \bar{Z} \tag{37}$$

where the last step follows because the average in (34) is nearly independent of m when $B/\Delta f \gg 1$, where Δf is the average separation between the zeros of $g(f,\theta)$. Thus

$$p_z(Z_m) = \frac{1}{\bar{Z}} \exp\left(-\frac{Z_m}{\bar{Z}}\right) \tag{38}$$

for all m.

Let us now assume that all jammers have the same power so that $J_m = J$ for all m. Then (32) becomes

$$R - \sigma^2 = J \sum_{m=1}^{M} Z_m. \tag{39}$$

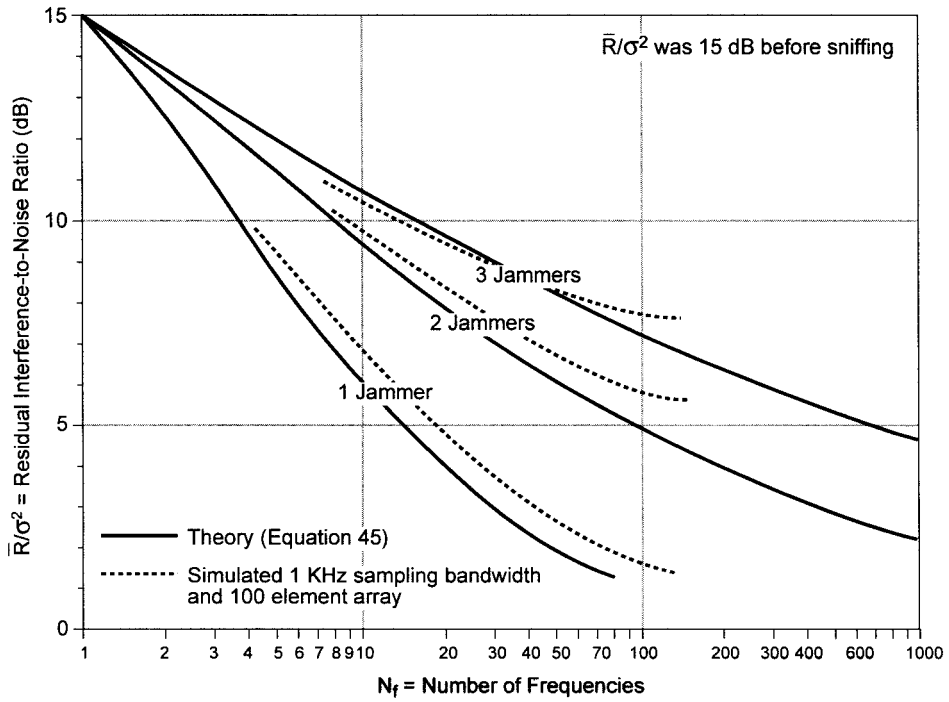

Fig. 3. Comparison of theoretical with simulated performance: simulated results are average of 20 random jammer distributions in far-out sidelobes.

If we now define

$$\rho = \frac{R - \sigma^2}{J} \tag{40}$$

to be the normalized total jamming power we obtain

$$\rho = \sum_{m=1}^{M} Z_m. \tag{41}$$

It is readily shown (using the characteristic function) that the probability density function for ρ is

$$p_\rho(\rho) = \frac{\rho^{M-1}\exp(-\rho/\bar{Z})}{\bar{Z}^M(M-1)!}. \tag{42}$$

The mean value of ρ is $\langle\rho\rangle = M\bar{Z}$ so that the probability that ρ is reduced to less than a fraction ε of its mean value is

$$\begin{aligned} P(\rho < \varepsilon M\bar{Z}) &= \int_0^{\varepsilon M\bar{Z}} \frac{\rho^{M-1}e^{-\rho/\bar{Z}}\,d\rho}{\bar{Z}^M(M-1)!} \\ &= \frac{1}{(M-1)!}\int_0^{\varepsilon M} t^{M-1}e^{-t}\,dt \end{aligned} \tag{43}$$

where $t = \rho/\bar{Z}$. Taking one sample of ρ from the distribution given in (42) corresponds to measuring the power at one of the N_f frequencies. Using the cumulative distribution in (43) the average number of frequencies for which ρ will be less than $\varepsilon M\bar{Z}$ is given by

$$\bar{N}_f = N_f P(\rho < \varepsilon M\bar{Z}). \tag{44}$$

Consequently, in order to get (on the average) one value (i.e., $\overline{N_f} = 1$) of ρ that is less than $\varepsilon\langle\rho\rangle = \varepsilon M\bar{Z}$ we require a number of frequencies N_f such that

$$N_f > \frac{1}{P(\rho < \varepsilon M\bar{Z})}. \tag{45}$$

Note that when the jammer portion of the power is reduced by ε the residual mean interference power including noise is

$$\bar{R} = \text{Residual Interference} = \varepsilon J\langle\rho\rangle + \sigma^2 \tag{46}$$

and the residual interference-to-noise ratio is

$$\bar{R}/\sigma^2 = \varepsilon\text{JNR} + 1 \tag{47}$$

where JNR is the total jammer-to-noise ratio due to all interferers. The reduction in interference-to-noise ratio in decibels is

$$\text{Reduction} = -10\log_{10}\left[\frac{\varepsilon\text{JNR}+1}{\text{JNR}+1}\right]. \tag{48}$$

III. Computer-Generated Results

A. Description of Computer Simulation

The sniffer was modeled on the computer to study its jammer nulling capability. Both linear and planar arrays were used in the study, but results will be presented only for the linear arrays. The performance of the sniffing technique operating on a planar array was approximately the same as that realized on a linear array. The element spacing was set to $0.58\lambda_o$ and a center frequency (f_c) of 5.0 GHz was used in all runs. A phase error, taken from a uniform distribution having an rms value of 2.9° (±5° peak error), was added to each element in all computer runs presented herein. Computer runs were also made using a 6° rms error per element. Performance using 6° was nearly the same as that obtained using 2.9°. The number of frequencies (N_f) sampled across the tunable bandwidth was varied from one to 128 in steps of powers of two. All jammers were assumed to spread their energy uniformly over the tunable bandwidth (constant power spectral density). The jammers were randomly distributed over a specified angular region and power measurements were made

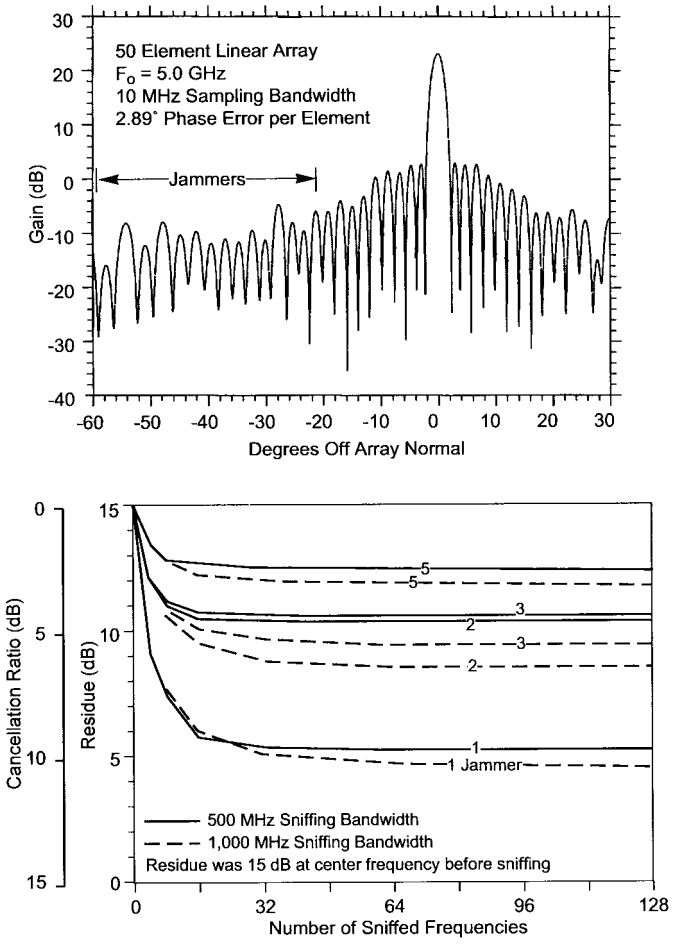

Fig. 4. Sniffer performance on 50-element linear array; phase shifters changed at each sniffed frequency; results are average of 20 random jammer distributions.

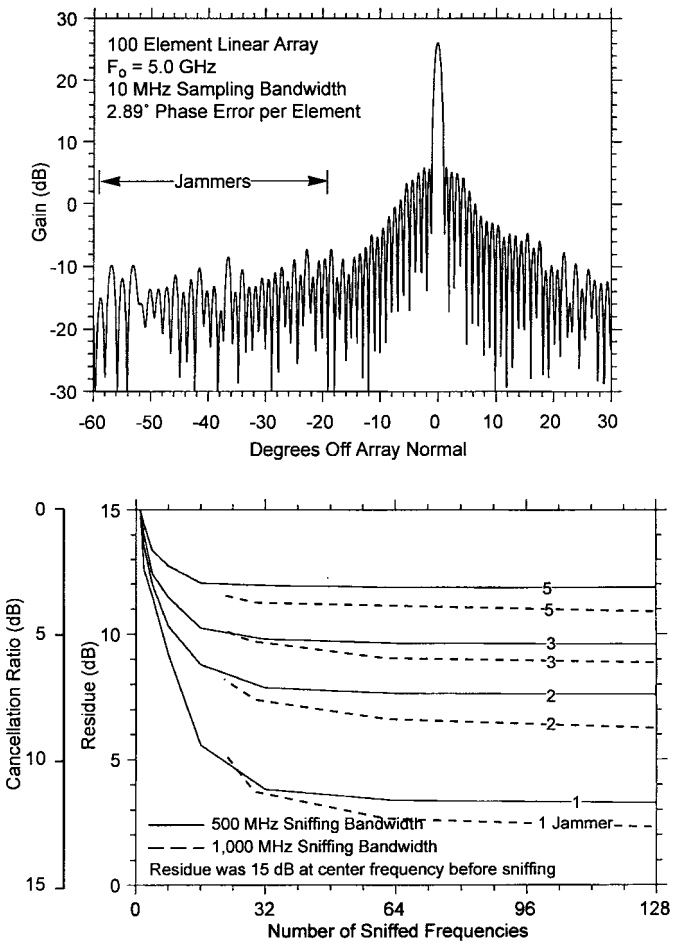

Fig. 5. Sniffer performance on 100-element linear array; phase shifters changed at each sniffed frequency; results are average of 20 random jammer distributions.

in a narrow sampling band (B_s) at equally spaced increments across the tunable band. A power measurement at a particular frequency f_i for a particular jammer constellation d was simulated by integrating over B_s, i.e.,

$$P_d(f_i) = P_n + J_o \sum_{j=1}^{N_j} \int_{f_i - B_s/2}^{f_i + B_s/2} |g(f, \theta_{jd})|^2 \, df \qquad (49)$$

where:

J_o	power spectral density of jammer received with isotropic gain;
$g(f, \theta_{jd})$	voltage gain of antenna pattern at angle θ_{jd} and frequency f;
θ_{jd}	angle of jth jammer in dth jammer constellation;
N_j	number of jammers.

The thermal noise (P_n) was set to unity and a sampling bandwidth of 10 MHz was used in most runs. The power measurement was repeated at each of the N_f frequencies and the smallest power was stored. The process was then repeated for 20 different jammer constellations and the average $(\bar{R})$ of the smallest powers was used as the performance measure, i.e.,

$$\bar{R} = \frac{1}{20} \sum_{d=1}^{20} [P_d(f_i)] \underbrace{\min}_{i=1,N_f} . \qquad (50)$$

The average residue-to-noise ratio over the Monte Carlo runs before operating the sniffer was obtained by setting f_i equal to f_c and N_f equal to one in (50). J_o was then scaled to force the average residue-to-noise ratio to always equal 15 dB before sniffing for each set of 20 jammer constellations. Fig. 3 compares the theoretical performance predicted by (45) with performance obtained from the computer simulation using (50) for a 100-element linear array. The sampling bandwidth was reduced to 1.0 kHz for comparison with the theoretical narrow-band analysis. The theoretical performance is observed to closely match the simulated performance.

Figs. 4–6 show simulated performance for 50-, 100-, and 200-element linear phase steered arrays. The antenna pattern and the angular region over which the jammers within each constellation were randomly distributed is also shown for each array. A sampling bandwidth of 10 MHz was used at each sniffed frequency when generating the results. Increasing the sampling bandwidth from 1 kHz to 10 MHz typically degraded the nulling performance by only about 1 dB.

The cancellation performance for all three arrays is observed to be roughly the same. The algorithm appears to require a sidelobe window having only a few nulls which it can shift around within the jammer cloud to minimize the interference. It is noteworthy that for a sniffing bandwidth of 1000 MHz,

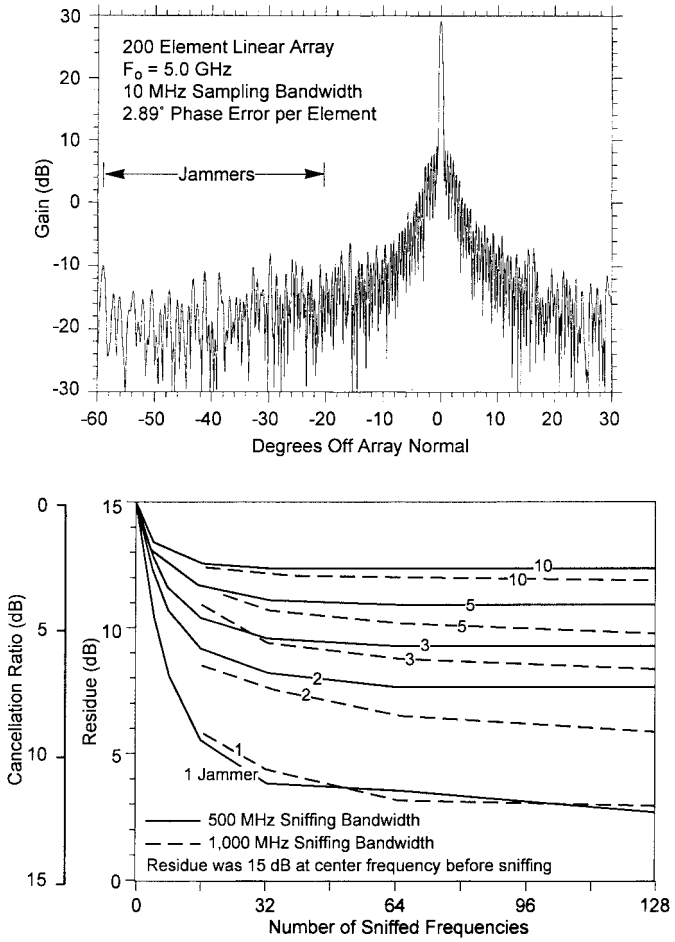

Fig. 6. Sniffer performance on 200-element linear array; phase shifters changed at each sniffed frequency; results are average of 20 random jammer distributions.

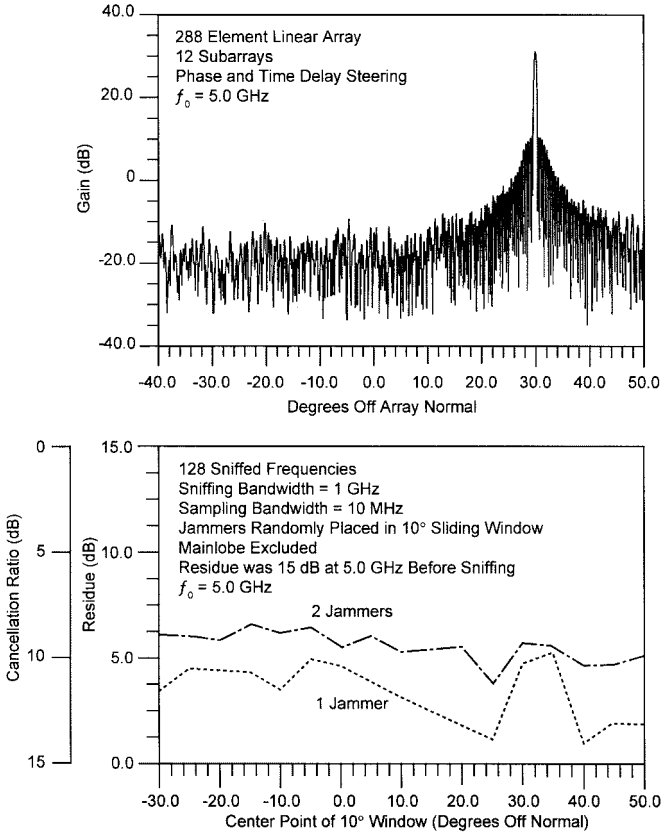

Fig. 7. Sniffer performance on a phase-time steered array results are average of 20 random jammer distributions.

the average time-bandwidth product (and the average number of nulls) for the 50-element array is only 2.2 over the 40-degree jammed sector, yet we still realize 6.5 and 5.5 dB of nulling against two and three jammers, respectively. The latter numbers increased to 8.7 and 6.2 dB for the 100-element array and 9.0 and 6.8 dB for the 200-element array. The few cases in Figs. 4–6 where a sniffing bandwidth of 500 MHz performed slightly better than 1000 MHz are apparently statistically anomalies (results were average of only 20 random jammer distributions).

Fig. 7 presents simulation results for a 288-element phase-time steered linear array. The array was divided into 12 subarrays each having 24 elements. Phase steering was used within each subarray and time steering was used to align the subarrays to each other. The array was phase and time steered to 30°. The antenna pattern is shown in the top insert. The curves in the bottom insert show performance sensitivity to the location of the interference. The jammers were randomly distributed within a 10° angular window whose location was varied in 5° steps relative to the beam pointing direction. The jammers were excluded from the mainlobe region (null to null) when creating the jammer constellations for the points centered at 25, 30, and 35°. The performance is observed to be roughly independent of the location of the jammers. The result may appear to be counter intuitive, since the time bandwidth product decreases as we approach the pointing direction. The explanation lies in the observation that even when the jammer is at 25°, BT' equals 2.5, i.e., even when the jammers are in the very near-in sidelobes, the sniffer has two nulls to choose from.

IV. Summary

The authors have demonstrated that significant jammer cancellation can be realized against multiple wide-band white noise, sidelobe jammers by intelligently selecting the operating frequency in a frequency agile radar or communication system. The proposed technique, called the sniffer, selects the frequency which places the jammers in or near nulls in their antenna sidelobe transfer functions. The number of available nulls for any given jammer is equal to its time-bandwidth product. Analysis and computer simulation predict that cancellation ratios typically vary between 12 and 3 dB as the number of sidelobe jammers varies between one and five.

References

[1] G. Petrocchi, S. Rampazzo, and G. Rodrguez, "Anticlutter and ECCM design criteria for a low coverage radar," in *Proc. Int. Conf. Radar*, Paris, Dec. 4–8, 1978, pp. 194–200.

[2] S. Strappaveccia, "Spatial suppression by means of an automatic frequency selection device," in *Proc. IEE Int. Conf. Radar'87*, Publication 281, London, U.K., Oct. 19–21, 1987, pp. 582–587.

Richard M. Davis (S'62–M'71–SM'85) received the B.S.E.E. degree from the University of Rochester, Rochester, NY, in 1964, and the M.S.E.E. and B.A. degrees from Syracuse University, Syracuse, NY, in 1968 and 1975, respectively.

From 1964 to 1965, he was with the IBM Systems Development Division, Communications Laboratory, Raleigh, NC. Between 1966 and 1990, he was with the Syracuse Research Corporation (SRC), Syracuse, NY. From 1984 to 1990, at SRC he was the Technical Director of the Analytical Studies Center which specializes in electronic counter countermeasures. He is currently a Principal Engineer with the MITRE Corporation in Bedford, MA. His research interests include signal and adaptive processing.

Ronald L. Fante (S'56–M'59–SM'72–F'79) received the Ph.D. degree from Princeton University, Princeton, NJ.

He has more than 35 years of experience in electromagnetics, optics, and signal processing.

Dr. Fante is a former Editor of the IEEE TRANSACTIONS ON ANTENNAS AND PROPAGATION and an IEEE Distinguished Lecturer. He is a Fellow of the Optical Society of America, and is listed in *Who's Who in America*.

Thomas P. Guella received the B.S. degree in physics and mathematics from Hunter College, New York, in 1977, and the M.S. and Ph.D. degrees in physics from New York University, New York, in 1980 and 1985, respectively.

From 1985 to 1989, he was a Technical Staff Member at the Massachusetts Institute of Technology Lincoln Laboratory, Lexington, where he was involved in adaptive algorithm and airborne radar development. Presently, he is a Lead Technical Engineer at the MITRE Corporation, Bedford, MA. His research interests include adaptive arrays and architectures, signal processing, pattern synthesis methods, and on-platform numerical modeling of airborne antennas.

Robert J. Balla received the B.S.E.E. degree from Virginia Polytechnic Institute, Blacksburg, in 1978.

From 1978 to 1983, he was employed as a Design Engineer for Hi-Rel military applications at Harris Corporation, Palm Bay, FL. From 1983 to 1988, he was the Senior Radar Systems Engineer for Kentron International, Kwajalein Missile Range, where he was responsible for improvement and modernization of the missile tracking radar systems. Since 1988 he has been with the U.S. Army Space and Missile Defense Command, Huntsville, AL, working on phased array, signal processing and countermeasure research and development for ground based radar systems.